

25-Gauge Instrumentation: Engineering Challenges and Tradeoffs

2

A.C. Barnes, C.M. DeBoer, P.R. Bhadri, O. Magalhaes Jr., R.M. Kerns, M.T. McCormick, L.P. Chong, M.S. Humayun

Core Message

- 25-gauge instrumentation has reduced the surgical incision size. This reduction in size has made vitreoretinal procedures not only sutureless but, more importantly, made the procedures less invasive and potentially safer.
- The sutureless 25-gauge pars plana vitrectomy reduces the postoperative inflammation at sclerotomy sites, thus reducing patient discomfort after surgery and hastening postoperative recovery.
- The majority of experienced vitreoretinal surgeons have now been exposed at some level to 25-gauge instrumentation, and many use it on a routine basis. However, only a few surgeons have experience with the engineering development challenges and tradeoffs associated with small-diameter instrumentation.
- This chapter will explore some of the key areas of the design and functioning of small-diameter instruments, so that surgeons may better understand their performance.

2.1 Introduction

25-gauge instrumentation refers to the body of devices designed specifically to work in conjunction with the 25-gauge Entry Site Alignment system (ESA) or microcannula system. The ESA system is the key to 25-gauge instrumentation, and allows the surgeon pars plana access to the vitreous chamber without having to perform conjunctival peritomy (i.e., transconjunctival access), and the ability to remove the system without the need for sutures [1]. The main components used with the ESA system include: a fiber optic light pipe, vitreous cutter, and a range of manipulation and task-specific instruments (Fig. 2.1).

The main advantage of 25-gauge instrumentation — and that which creates engineering challenges — is the dimensional constraint of instruments 0.5 mm in diameter. Compared to 20-gauge, 25-gauge instruments have 70% less cross-sectional area to recreate the functionality surgeons expect (Fig. 2.2). This chapter will explore how the size of 25-gauge instrumentation affects mechanical properties, such as fluid dynamics and stiffness, and optical properties associated with illumination. As engineering solutions to these challenges continue to be developed, transconjunctival 25-gauge instrumentation will continue to improve as well.

Currently, there are at least four major brands of 25-gauge instrumentation Bausch and Lomb Inc. (St.

Louis, MO, USA), Alcon Laboratories, Inc (Fort Worth, TX, USA), Dutch Ophthalmic, USA (Kingston, NH, USA), Synergetics Inc. (O'Fallon, MO, USA), as well as others) (Fig. 2.3). There are differences between these systems that affect their performance, and some of these will be highlighted. But, as designs evolve and new instrumentation is launched, the comparative landscape is constantly in flux. The goal of this chapter is to provide information on how the design parameters of 25-gauge instruments affect their performance, so that surgeons are better prepared to evaluate and operate current and future instrumentation. For example, 23-gauge instrumentation systems for use with tunneling scleral incisions are just beginning to be evaluated and compared to 20 and 25-gauge instrumentation [9]. Journal articles, conference presentations, and manufacturer information highlighting various comparisons may lead to confusion. Hopefully, this chapter will allow a better understanding of the underlying scientific reasons behind any performance differences.

2.2 Microcannula System

The 25-gauge Entry Site Alignment system (ESA) is the primary component of 25-gauge instrumentation. The ESA system establishes the pars plana transconjunctival

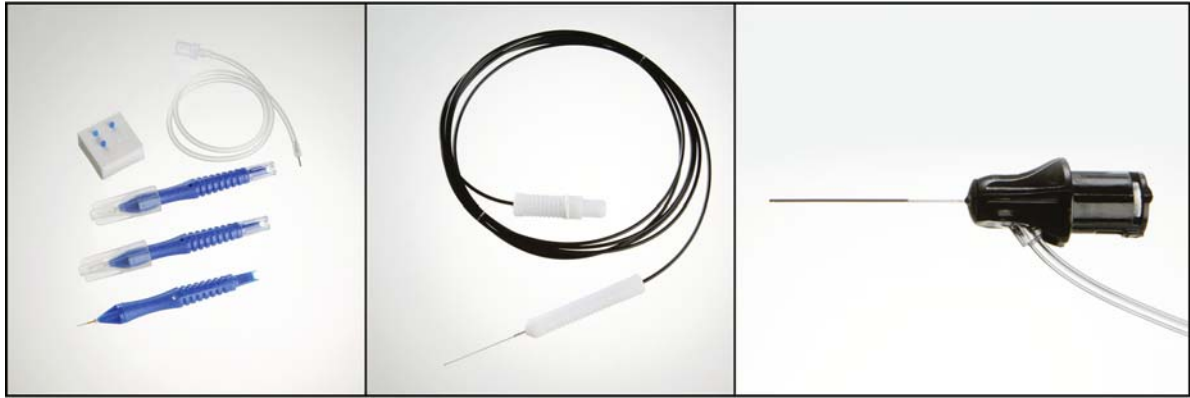


Fig. 2.1 Main components of 25-gauge instrumentation

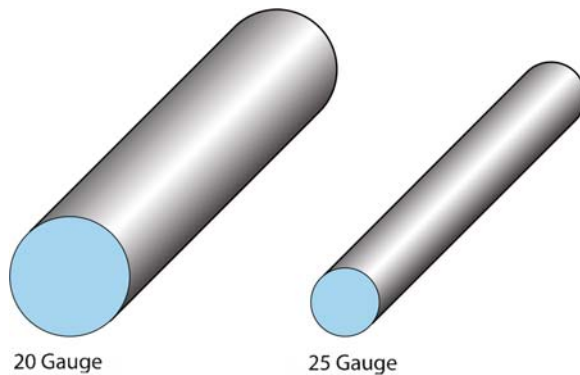


Fig. 2.2 Comparison of cross-sectional areas (20-gauge vs. 25-gauge)

entry ports into the vitreous chamber, and provides access for the balance of the 25-gauge instruments. As the name suggests, the ESA system serves to maintain alignment between the entry holes in the conjunctiva and sclera, as well as provide unobstructed instrument access. This is especially important due to the small size of 25-gauge wounds and the technique of conjunctival displacement prior to the insertion of the ESA system. While microcannula systems are optional for 20-gauge instrumentation, it is not recommended to attempt

25-gauge cases without the use of the ESA system. It is not feasible to attempt to locate and align 25-gauge conjunctival and scleral entry ports each time an instrument is inserted.

The ESA system components include: the 25-gauge trocar-mounted microcannulas, cannula plugs, and infusion line (Fig. 2.4). The microcannulas are preloaded on the 25-gauge needle trocars and the combined components of the trocar needle, microcannula, and trocar handle is referred to as the trocar/cannula assembly. The trocar handle allows the surgeon to securely grasp the assembly during insertion. Some trocar handles provide advanced features such as built-in marking calipers for consistent cannula placement within the pars plana.

The microcannulas consist of two components: a polyimide cannula and a polymer cannula hub. The polyimide cannula is mounted within the polymer hub or collar. The cannula forms the entry port, and utilizes a distal bevel to facilitate insertion through the tissue. The polyimide cannula material provides both strength and flexibility, allowing the cannula wall to be thin and to avoid collapsing or buckling. The hub maintains the position of the cannula, and prevents it from sliding too far into the vitreous chamber. In addition, the hub allows



Fig. 2.3 25-gauge microcannula systems from various manufacturers

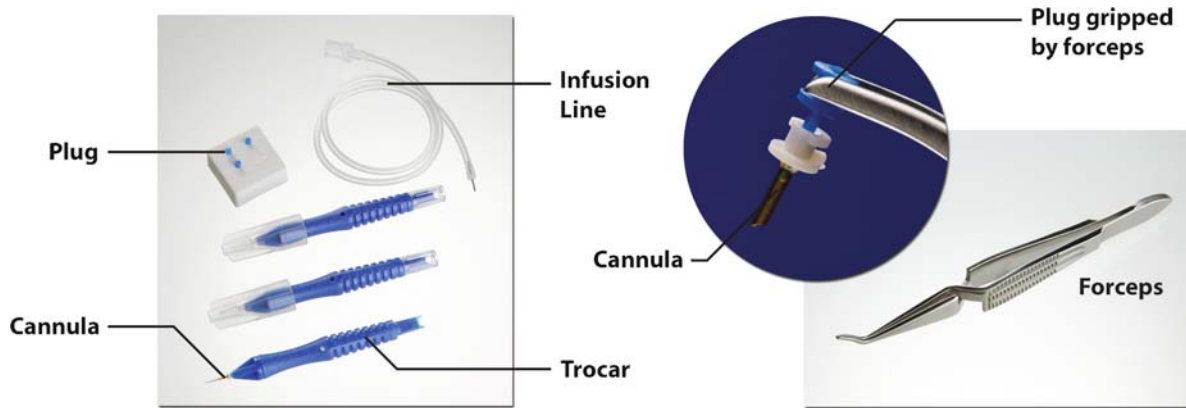


Fig. 2.4 25-gauge Entry Sight Alignment system components

surgeons to grasp the cannula, and provides an entry funnel to assist during instrument insertion.

The cannula plug is used to seal the cannula after insertion into the eye wall. It is designed with a tapered shaft or a tight sliding fit to seal within the cannula port. The plug should be inserted only as far as necessary to seal the cannula. Forcing the plug too far within the cannula may cause problems during removal. Even with proper plug insertion, counter-force should be applied to the cannula hub when removing a plug. Both the plug and the cannula hub are designed to facilitate manipulation using standard ophthalmic forceps or specialized scleral plug forceps. The infusion line is designed to have a tight sliding fit within the cannula port, and provides a standard female Luer-lock adapter on the proximal end of the tubing. The infusion line may be relocated to any available cannula as necessary.

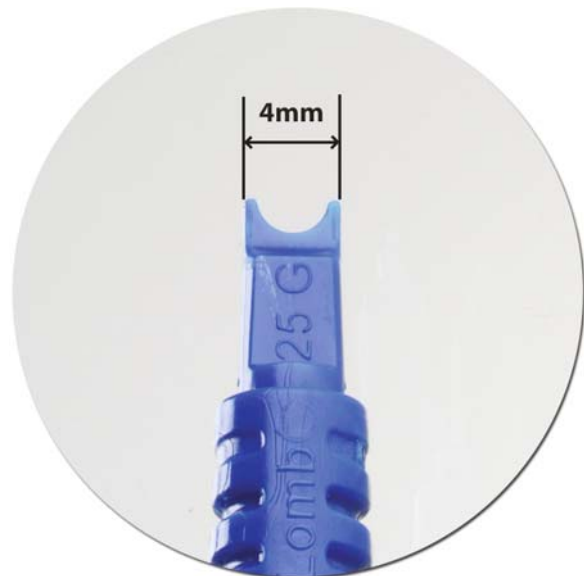


Fig. 2.5 Integrated scleral markers

2.3 Entry

The ESA system is designed to transconjunctivally insert the 25-gauge microcannulas within the pars plana. Entry points may be indicated with standard calipers or, for some systems, utilizing the integrated scleral markers (Fig. 2.5). These markers provide three possible measurements. The distance between the centers of each marker is 3.5 mm, while the distance from each outside edge and each inside edge is 4.0 mm and 3.0 mm respectively.

The performance of the trocar/cannula insertion (Fig. 2.6) is influenced by a number of factors and forces, including: the trocar needle puncture, sliding friction, cannula insertion, and the overall size of the wound. The initial puncture which begins the insertion process is accomplished when the distal end of the trocar needle tip applies enough pressure to cause the tissue structure to fail or displace. Various parameters play a role during the initial puncture,



Fig. 2.6 Trocar/cannula insertion

including the size of the trocar point (sharpness), the tissue condition, and the intraocular pressure. The total force applied to the trocar handle to initiate the puncture is affected by the trocar point size and the state of the patient's tissue. The pressure necessary for puncture is dictated by the composition of the tissue, while the total force needed to reach this pressure is governed by the area of the trocar point (pressure = force per unit area).

For the trocar to reach the critical puncture pressure, the tissue must oppose the applied force. The tissue at or near the puncture site will usually deflect prior to fully opposing the applied trocar force. The amount of deflection is affected by the tissue and the intraocular pressure. As the tissue deflects away from the trocar point, the intraocular volume is reduced and the intraocular pressure increases until it opposes the trocar force. This allows the point pressure to rise until the tissue is punctured. Lower initial intraocular pressure may allow greater eye wall deflection prior to trocar puncture. To minimize eye wall deflection and intraocular pressure spikes during trocar/cannula insertion, the trocar needle should have a sharp undamaged point.

Once the trocar point punctures, the trocar side bevels begin to slice and enlarge the wound so that it may accommodate the trocar shaft. As the trocar enters, the wound tissue exerts a normal force on the trocar surface. This force provides sliding resistance or friction based on the frictional coefficient and surface area of the shaft. The sliding friction may be improved by reducing the frictional coefficient of the trocar shaft.

The next critical event during the trocar/cannula entry is the insertion of the polyimide cannula into the wound

created by the trocar. The distal end of the cannula is cut at approximately a 30° angle to assist the introduction of the cannula into the wound. The bottom bevel cut introduces a small portion of the cannula into the wound, and allows the wound to progressively stretch to accommodate the full cannula diameter. This feature minimizes the potential for the leading edge of the cannula to catch on tissue, which may result in increased insertion force and cannula buckling. When this situation is encountered during cannula insertion, the tendency is to apply more force which may exacerbate the problem. Decreasing insertion pressure and slightly withdrawing the trocar/cannula can allow any tissue caught on the cannula to be dislodged prior to proceeding with the cannula insertion.

One metric that impacts cannula insertion into the trocar wound, as well as cannula performance during the case is the Trocar/Cannula Delta (T/C Delta). The T/C Delta provides a measure of the gap between the outer diameter of the trocar and the inner diameter of the cannula (Fig. 2.7).

The larger the T/C Delta, the more the trocar wound has to stretch to accommodate the cannula, and the greater the risk of tissue incarceration into the T/C gap during cannula insertion. The increased insertion force associated with the cannula becoming caught on tissue can cause greater eye wall deflection, increased intraocular pressure, and potential cannula buckling. Obviously, it is important to minimize the T/C Delta, just as it is important to maintain a sharp trocar point.

As with most design parameters, there are trade-offs associated with the T/C Delta. First, the T/C Delta

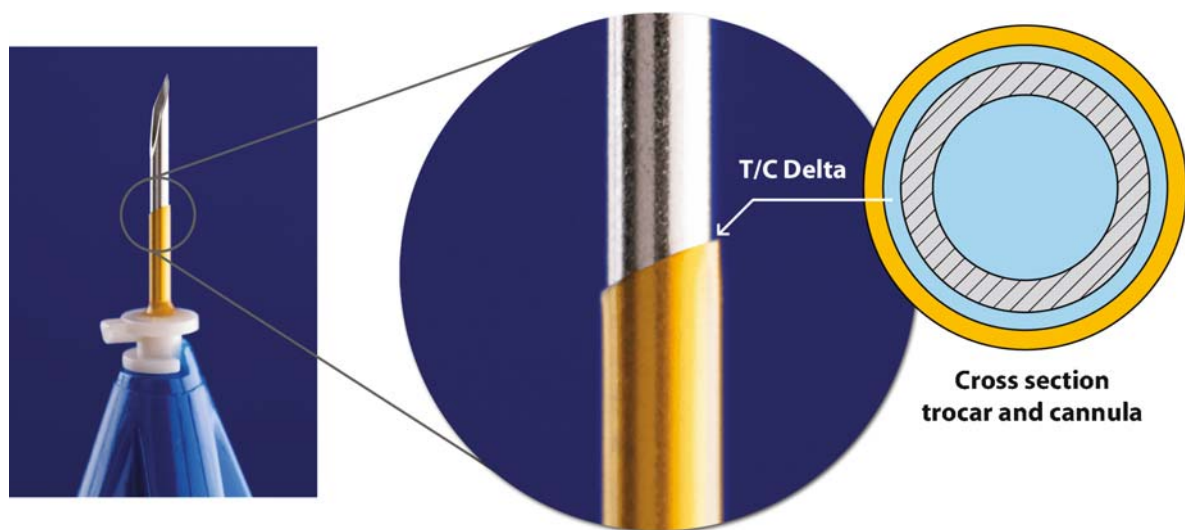


Fig. 2.7 Illustration of Trocar/Cannula Delta

provides a measure of how easily the cannula is able to slide relative to the trocar shaft. If the T/C Delta is too small, the cannula insertion will be smooth but it may be difficult for the surgeon to remove the trocar from the cannula. A large trocar handle force and a large cannula counterforce may be necessary to remove the trocar. As the trocar slides free of the cannula under a large retraction force, the surgeon's hand can accelerate away from the eye, leading to a number of adverse events, including: contact with non-sterile portions of the surgical microscope, contact with or sticking of the needle to the assistant or self, or over-compensation leading to an inadvertent sticking of the trocar to the patient's eye. Secondly, the T/C Delta governs the extent the wound stretches to accept the cannula and thus the normal force applied to the outer surface of the cannula. This normal force affects both the amount of friction holding the cannula in place during the case, and the amount of force required for cannula removal at the conclusion.

A T/C Delta that is too small may allow an easy insertion, but may not provide enough wound holding force to prevent inadvertent cannula removal during the case. Too large a T/C Delta may lead to large insertion forces, cannula buckling, and large cannula removal forces.

2.4 Infusion

Each ESA system includes a cannula-based infusion line with a female Luer-lock connector, to allow a secure connection to the balanced salt solution (BSS) infusion tubing and bottle (Fig. 2.8). The infusion cannula is designed to have a precise sliding fit within the microcannula. This allows insertion by the surgeon, but provides enough friction to prevent ejection of the line during the case.

If necessary, the infusion line may be relocated to any microcannula.

The role of the infusion cannula is to maintain the intraocular pressure at the level selected by the surgeon via the microsurgical system. The infusion cannula must provide adequate volume flow rate to maintain this pressure while fluid is being removed from the eye either by aspiration or leakage [3]. A more detailed discussion of fluid dynamics is covered in the Fluid Dynamics Sidebar. The relationship between the various parameters established in the sidebar will be utilized in the fluidics discussion relating to the infusion line and the vitreous cutter.

The cannula-based infusion line of the ESA system is similar to its 20-gauge counterpart until about the last centimeter. The extension line, Luer connector, stop-cock, and BSS bottle connection tubing are substantially equivalent for both 25 and 20-gauge infusion lines. The difference is found relatively close to the eye in the size of the infusion cannula. (Note: some early 25-gauge infusion line extension tubing was significantly smaller than that of a 20-gauge line and could affect flow, but for this chapter, extension line effects will be assumed similar to 20-gauge) As one would expect, and may be seen in the Fluid Dynamics Sidebar, the smaller inner diameter of the 25-gauge infusion cannula provides greater flow resistance than 20-gauge infusion cannulas. To generate a volume flow rate similar to that of a 20-gauge infusion cannula, the 25-gauge cannula requires a greater pressure differential. In addition, from the continuity equation, the flow velocity of the 25-gauge cannula will be higher at the same volume flow rate, due to the smaller cross-sectional area.

The lower average volume flow rate associated with the small size of the 25-gauge infusion cannula is balanced by the corresponding increase in flow resistance of the

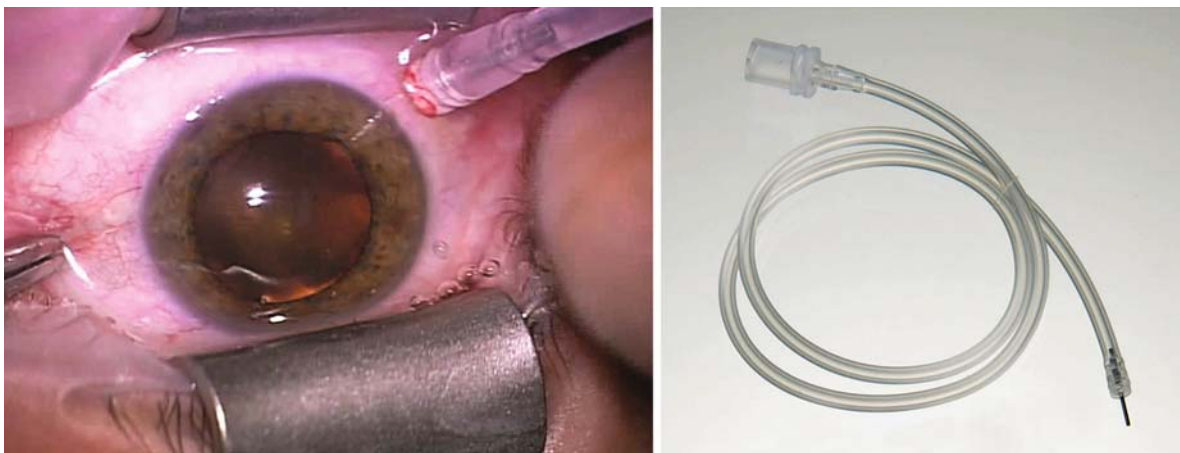


Fig. 2.8 25-gauge cannula based infusion line

vitreal cutter. During 25-gauge vitrectomy, the infusion cannula is not required to deliver the volume flow rate needed for a 20-gauge case. In general, 25-gauge cases require less BSS than 20-gauge cases, due to reduced fluid turnover during 25-gauge vitrectomy and minimal leakage from the ESA system.

The principles of infusion can be used to understand procedures like air/fluid exchange. In this situation, the infusion enters the eye and directly impacts the retina. This has been shown to cause damage [10–13]. As the velocity of the infusion increases, more pressure is applied to the retina, which may increase damage. As discussed above, the smaller diameter of the 25-gauge infusion cannula can generate higher velocities, potentially increasing the force on the retina. The infusion parameters should be adjusted to minimize these effects. One possible solution is an atraumatic infusion cannula, which perturbs the infusion flow as it enters the eye [14].

Summary for the Clinician

- Entry Site Alignment system (ESA is the key to 25-gauge instrumentation).
- The ESA system serves to maintain alignment between the entry holes in the conjunctiva and sclera, as well as provide unobstructed instrument access. It is not recommended to attempt 25-gauge cases without the use of the ESA system.
- The performance of the trocar/cannula insertion is influenced by a number of factors and forces, including: the trocar needle puncture, sliding friction, cannula insertion, and the overall size of the wound.
- The infusion cannula is designed to have a precise sliding fit within the microcannula. This allows insertion by the surgeon, but provides enough friction to prevent ejection of the line during the case. If necessary, the infusion line may be relocated to any microcannula.
- The lower average volume flow rate associated with the small size of the 25-gauge infusion cannula is balanced by the corresponding increase in flow resistance of the vitreal cutter.

2.5 Fluid Dynamics Sidebar

Surgeons encounter many critical intraoperative situations when they have to determine appropriate infusion and aspiration variables. With knowledge of the

relationships between the various parameters, a surgeon will be better equipped to adjust the flow settings for the desired outcome, and will understand how 25-gauge instrumentation differs from 20-gauge. This sidebar is intended to give a more detailed description of the underlying fluid dynamics governing infusion and aspiration flow. It is not a complete tutorial for fluid dynamics. The equations are shown to highlight the relationships between flow variables, and may not provide a full description of the flow situation, boundary conditions, and assumptions necessary to apply the equations directly.

Rolf H. Sabersky et al. describes a fluid as “A substance that, when at rest, cannot sustain a shear force (that is, a force exerted tangentially to the surface on which it acts).” [15] The fluid in this case is primarily BSS, or water, an incompressible viscous fluid. One of the principal equations governing incompressible fluid flow is the continuity equation. This equation is a result of mass conservation, and may be applied to incompressible fluids. It states that for a control volume, the net flux of fluid into the volume is equal to the net flow out. The mass flow rate into or out of a pipe, which is constant, may be taken as the fluid density multiplied by the fluid velocity times the area of the pipe:

$$\text{Mass flow rate} = \rho \cdot V \cdot A = \text{Constant}$$

The volume flow rate (Q) may be obtained by dividing through by the fluid density, and the continuity equation may be used to compare the velocity at one point in a tube to another point.

It may be seen in Fig. 2.9 that the cross-sectional area and velocity are inversely proportional. As the area of the cross-section increases, the velocity decreases. For the same volume flow rate, a smaller diameter tube will produce a higher velocity fluid flow. Therefore, as instrumentation becomes smaller, larger flow velocities are required to maintain comparable volumetric flow rates to larger systems.

While the continuity equation may be used to describe the velocity in tubing with varying diameters, the Bernoulli equation may be used to describe flow into and out of the eye. The Bernoulli equation is typically used to describe an inviscid, incompressible fluid moving along a streamline from point A to point B. Bernoulli's equation states that the total energy (or head) along the streamline remains constant. It shows the relationship between the three main forms of head: velocity head, gravity head, and pressure head.

$$\text{Bernoulli equation: } \frac{V^2}{2} + gh + \frac{P}{\rho} = \text{Constant}$$

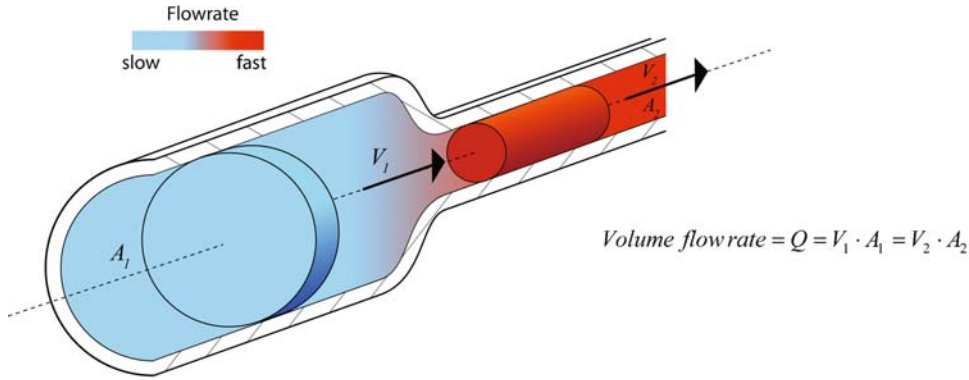


Fig. 2.9 Volume flow rate in a pipe

where:

V = fluid velocity

g = gravitational acceleration

h = height above a datum point

p = pressure

ρ = fluid density

For viscous fluids, such as BSS, some of the energy of the fluid is transferred out as heat, and loss terms, or viscous head, must be added to the equation. Substituting in the variables associated with infusion into the eye, the

$$\frac{V_{\text{bottle}}^2}{2} + gh_{\text{bottle}} + \frac{p_{\text{bottle}}}{\rho_{\text{BSS}}} + \text{Losses} = \frac{V_{\text{eye}}^2}{2} + gh_{\text{eye}} + \frac{p_{\text{eye}}}{\rho_{\text{BSS}}}$$

equation becomes:

The losses due to friction, transitions, or diameter changes of the infusion line are on the left hand side of the equation. To simplify the equation, a number of terms may be canceled. The fluid in the bottle is near stationary, and therefore V_{bottle} is approximated as zero. The height of the eye is typically chosen as the datum level, and therefore h_{eye} is zero relative to the bottle (the bottle height is referenced off the eye).

$$gh_{\text{bottle}} + \frac{p_{\text{bottle}}}{\rho_{\text{BSS}}} + \text{Losses} = \frac{V_{\text{eye}}^2}{2} + \frac{p_{\text{eye}}}{\rho_{\text{BSS}}}$$

From this equation it is evident that the height of the bottle or the pressure in the bottle provides the driving force for the intraocular pressure. To drive the flow into the eye, either the pressure in the bottle (e.g., VGFI) or the bottle height (e.g., IV pole) can be increased.

The losses on the left hand side of the equation are dependent on flow; as the flow velocity reaches zero so

do the loss terms, resulting in the hydrostatic pressure equation for an incompressible fluid.

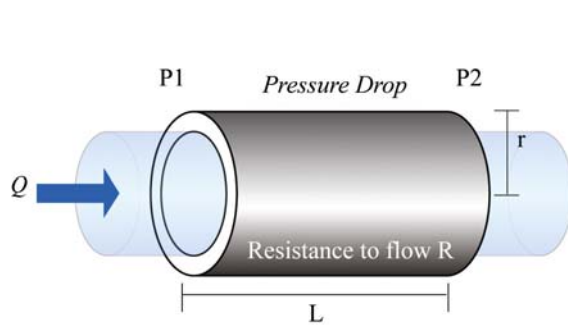
$$p_{\text{bottle}} - p_{\text{eye}} = -\rho_{\text{BSS}} gh_{\text{bottle}}$$

In general, the viscous head is a function of the fluid velocity, tubing diameter, and position along the streamline (viscous head builds or integrates as it removes head from the other terms). It is also scaled by the tube or pipe friction factor, which depends on the Reynolds number and the roughness of the tube surface. For low Reynolds number laminar flow, such as that encountered in the infusion line, the friction factor depends solely on the Reynolds number. For more detailed information on the viscous loss terms, consult your favorite fluid dynamics reference.

While the Bernoulli equation describes how fluid moves along a streamline, Poiseuille's law describes the volume flow rate of an incompressible viscous fluid through a tube of constant circular cross-section. This equation may be derived from the Bernoulli equation by accounting for frictional losses (which are solely a function of Reynolds number in laminar flow).

Poiseuille's law illustrates the key relationships between the flow parameters and volume flow rate. In particular, note the strong influence of the inner radius on flow. If the inner radius is reduced by half, the volume flow rate decreases by a factor of sixteen. The remaining terms show that the volume flow rate is directly proportional to the pressure differential, while inversely proportional to the fluid viscosity and the length of tube (Fig. 2.10).

The principal differences between the 25- and 20-gauge infusion line and vitreous cutter are found at the distal tubes (cannulas) that enter the eye. Poiseuille's law may be used to illustrate the increased driving force required for smaller diameter instruments. When the inner diameter



$$Q = V \cdot A = V \pi r^2 = \frac{\Delta P \cdot \pi r^4}{8 \eta L}$$

where:

Q = volume flow rate

V = fluid velocity

A = cross-sectional area

r = inner radius

ΔP = pressure differential

η = fluid viscosity (*dynamic*)

L = length

Fig. 2.10 Poiseuille's law



Fig. 2.11 25-gauge vitreous cutter tip



Fig. 2.12 Vitreous demonstrating solid characteristics

of the instrument is reduced, a larger pressure differential is required to maintain equivalent flow rates. For example, in 25-gauge vitrectomy cases, higher pressures are typically required to produce similar flow rates to corresponding 20-gauge procedures.

2.6 Vitreous Cutter

25-gauge vitreous cutters are designed to function through the ESA microcannula system (Fig. 2.11). They are currently available as high-speed guillotine-style cutters, driven either electrically or pneumatically. Other

than their size differences, current 25-gauge vitrectomy cutters are the same as their 20-gauge counterparts, and operate at similar cut rates.

Unlike the infusion cannula, the vitrectomy hand-piece is used in both vitreous and BSS (as well as other intraocular solids and fluids). BSS is a fluid, and obeys fluidics laws such as the Bernoulli equation. In contrast, vitreous is not a fluid. This may seem counterintuitive, as it is aspirated in a similar manner to BSS and does flow through the lines. When considered a little more, it becomes more evident. It is primarily water (98%), with the remaining material (2%) consisting mainly of collagen, hyaluronic acid (HA) and other noncollagenous

proteins and glycoproteins. This remaining matrix of material accounts for the gelatin-like structure of vitreous, which allows it to sustain a shear force (Fig. 2.12).

In order to remove vitreous, aspiration is not enough. As vitreous is aspirated into the cutter port, the cutter blade extends across the port and sections off a portion of the vitreous. This portion of vitreous, in suspension with BSS, can then travel through the aspiration line as the cutter begins the next cut.

Although the flow through the vitrectomy cutter is more complex than the infusion flow, many of the concepts are similar, especially if BSS flow is considered. When considering BSS flow, the constraints that apply to the infusion line are also applicable to the aspiration line. Aspiration flow may be modeled with the Bernoulli equation (see: Fluid Dynamics Sidebar). The difference between the eye pressure and microsurgical system vacuum pressure supplies the driving force for aspiration. Thus, higher vacuum pressure and/or greater intraocular pressure (i.e., a higher infusion pressure) will result in a higher flow rate.

In order to maintain eye pressure, the infusion line must be able to deliver flow at a higher rate than the cutter's aspiration rate and leakage losses. If the aspiration rate is greater than the infusion rate, hypotony and its related risks (choroidal hemorrhage, retinal contact, etc.) may result. If the eye pressure is too high, blood flow to the eye will stop and retinal damage may occur. Therefore, it is critical to maintain adequate pressures and provide a "safe zone for vitrectomy."

During 25-gauge vitrectomy, the infusion cannula is not required to deliver the volume flow rate needed for 20-gauge cases. The vitrectomy cutter tip provides a smaller aspiration diameter than the infusion cannula, due to the two-cannula design. The outer housing provides the tip structure, as well as the distal port for vitreous to enter the cutting chamber. The inner cannula slides within the outer housing, and provides the guillotine action used to cut the vitreous. Aspiration occurs when fluid and material flow into the outer housing and through the inner cannula. Therefore, the inside diameter of the inner cannula dictates the flow characteristics. While the outer tip housing is 25-gauge, the inner tip is smaller. For example, 25-gauge cutters can have an inner tip that is approximately 30-gauge. From the Fluid Dynamics Sidebar, Poiseuille's law shows that flow is proportional to the fourth power of the radius. This indicates that the inner cutter will have greater flow losses than the infusion cannula. Furthermore, the inner cutter is longer than the infusion cannula, further increasing flow friction (and decreasing flow rate). The increased flow losses associated with smaller diameter cutters require higher

pressure differentials for aspiration. For 25-gauge cases, an aspiration vacuum setting of 550 mmHg is a typical operating parameter.

2.6.1 Drive Mechanism

There are three major types of drive systems used for vitrectomy handpieces: guillotine electric, guillotine pneumatic, and reciprocating rotary pneumatic. The first type is an electric drive with a sinusoidal transmission which is currently used for both 20- and 25-gauge instruments. The sinusoidal transmission translates the rotary motion of an electric motor shaft to the linear guillotine motion of the inner cutter tip. The drive contains a ball bearing that rides in a sinusoidal track. The position of the ball bearing is constrained, yet the ball is free to rotate. As the sinusoid cam rotates with the motor, the ball follows the track and forces the ball housing to linearly translate, raising and lowering the cutter (Fig. 2.13). The profile of the motion remains constant (although faster) as cut rate is increased. Thus, the duty cycle (ratio of time the cutter port is open or closed) remains constant as the cut rate is increased and decreased. One can think of the motion profile as a sinusoidal wave of increasing or decreasing frequency (cut rate), but of constant amplitude.

Pneumatically driven cutters use air pulses provided by the surgical system to extend the cutter tip. The first type of pneumatic cutter is a guillotine-type cutter (Fig. 2.14). The cutter tip is attached to a diaphragm. When the surgical system provides an air pulse, the diaphragm is extended and the cutter tip closes, completing a cut. When air is released, a spring returns the tip to the open position. This closing and opening has a characteristic constant time. As cut rate is increased, the duration of open time per cut decreases, while the closed time remains constant. This causes the total fraction of time the cutter port is open over the time it is closed to decrease as cut rate is increased (decreasing duty-cycle). Furthermore, some systems have been shown to stop opening completely as speed increases. This is not typical for most pneumatic cutters.

The second type of pneumatic drive mechanism utilizes a dual drive line system. The surgical system supplies intermittent air pulses, alternating between each line. The first drive line acts to close the port, while the second line opens the port. The mechanism is shown in Fig. 2.15. Air pulses from the dual line system are supplied to either side of a horizontal piston, and act to move the piston laterally from side to side. A gear rack attached to the piston meshes with a geared section of the inner cutter. As the piston moves from side to side, the inner cutter tip reciprocates in a radial fashion. With this mechanism, the

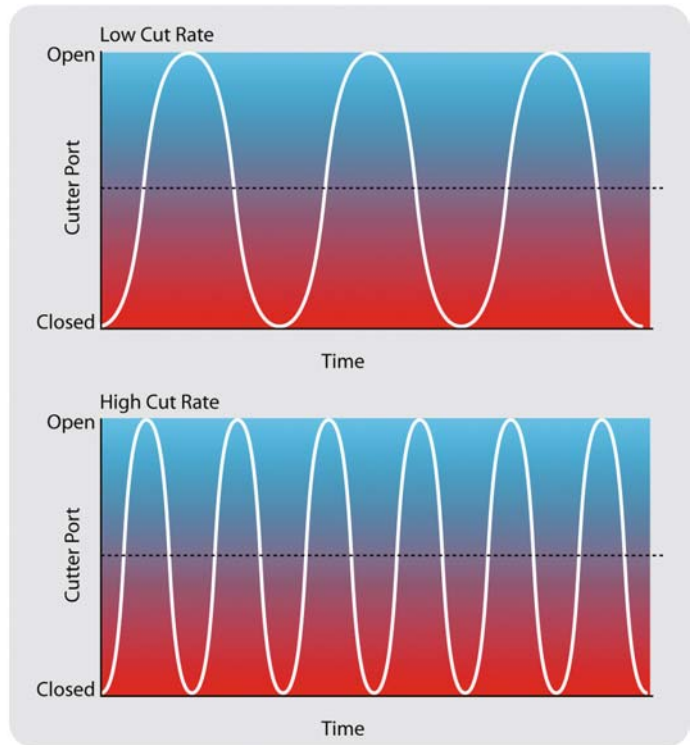
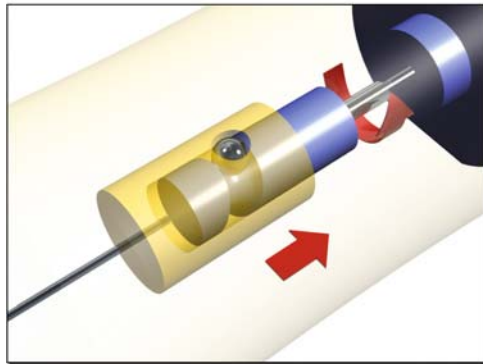
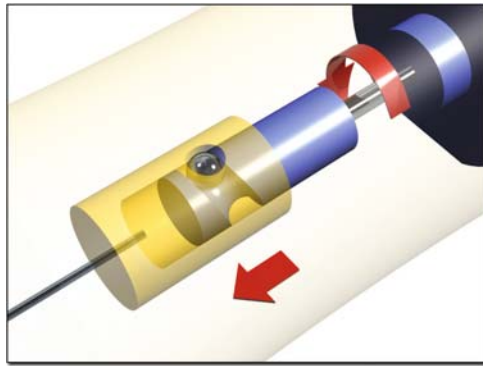


Fig. 2.13 Guillotine electric drive mechanism with sinusoidal cam

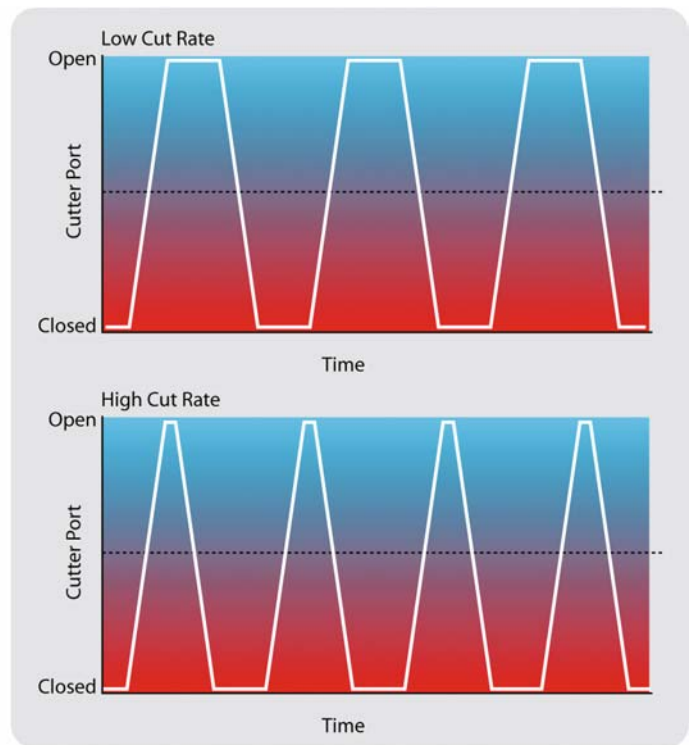
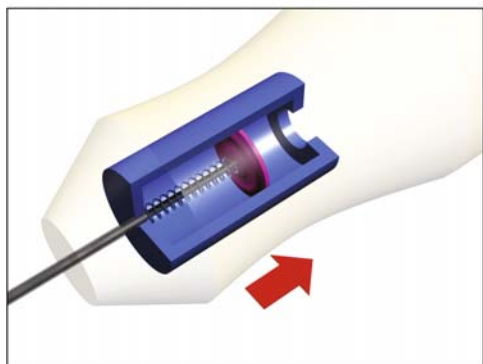
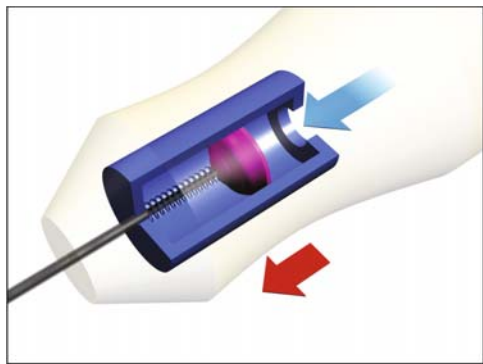


Fig. 2.14 Guillotine pneumatic drive mechanism with spring return

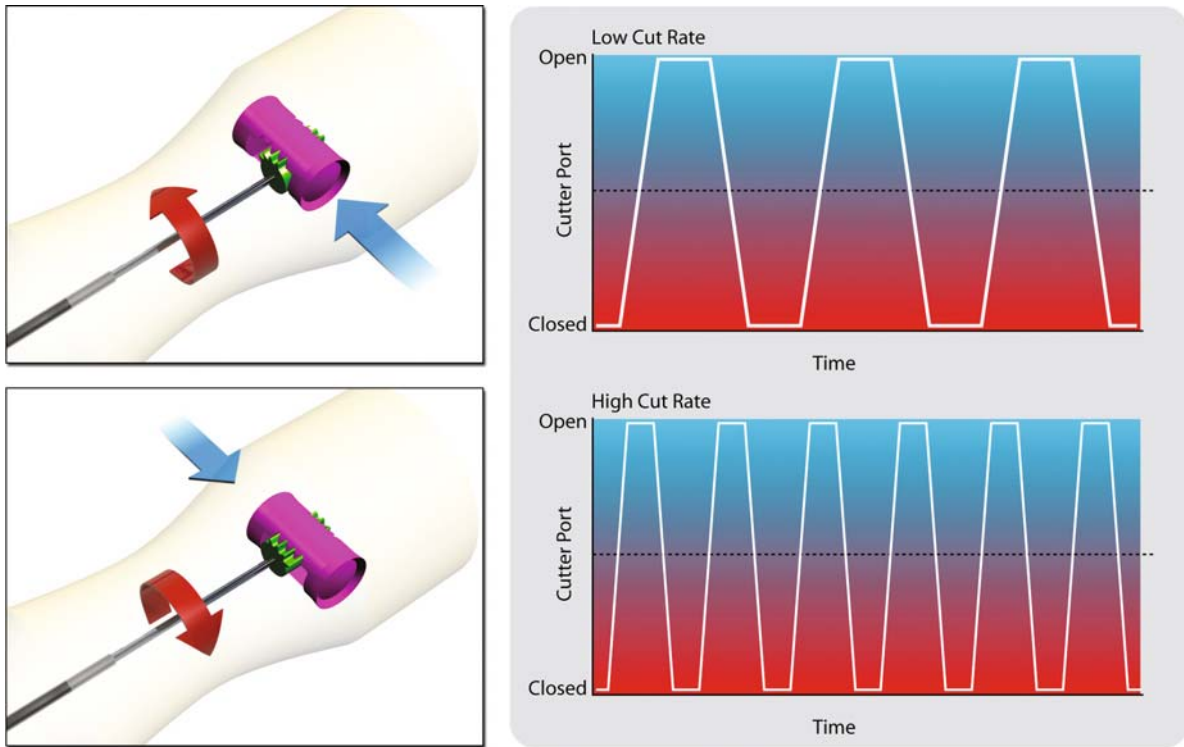


Fig. 2.15 Reciprocating rotary pneumatic drive mechanism with dual drive lines

cutter can maintain a constant duty-cycle. This type of pneumatic drive is currently only used on 20-gauge vitrectomy cutters.

2.6.2 Flow Rate

Vitreous cutter flow rates in BSS and in vitreous have been shown to be different [16]. Flow rates in BSS are indicative of the duty cycle of the cutter. Constant duty cycle electric cutters demonstrate constant flow rates in BSS as cut rate varies. However, for 25-gauge electric cutters, vitreous flow increases as cut rate increases. This has been demonstrated with the 25-gauge Bausch

& Lomb Lightning cutter. For single drive line, spring-return pneumatic cutters, the duty cycle and BSS flow decreases as the cut rate increases. For this type of guillotine pneumatic cutter, vitreous flow follows the BSS trend and also decreases with increasing cut rate. This has been demonstrated with the 25-gauge Alcon Accurus cutter (Table 1, Fig. 2.16).

2.7 Traction

Traction is an important dynamic of vitrectomy. It is the pulling force that is applied to tissue due to aspiration flow. Traction is necessary for vitreous and other material

Table 2.1 25-gauge cutter flow rates at 550 mmHg aspiration

25-gauge Accurus and B&L flow characteristics in porcine vitreous (ml/s)			
	600 cpm	1,000 cpm	1,500 cpm
Alcon Accurus	0.013	0.013	0.006
B&L Lightning	0.008	0.012	0.014

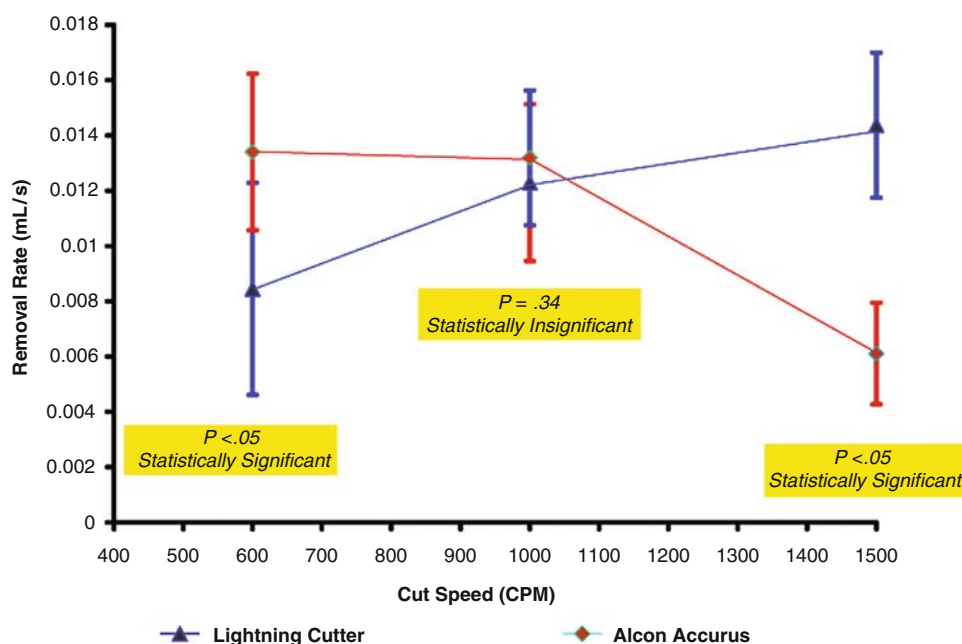


Fig. 2.16 25-Gauge lightning cutter and alcon accurus removal rates of porcine vitreous

to enter the cutter port, but should be maintained at a safe level. This is especially critical when cutting next to the retina. High traction forces may lead to small retinal tears, possibly resulting in retinal detachment.

Traction is a complex relationship between the cutter port pressure differential, the port configuration, aspiration flow, cut speed, vitrectomy cutter movement, and the nature of the tissue (e.g., the ratio of fluid to tissue or the degree of tissue connectivity). Traction is typically controlled by the surgeon varying aspiration pressure, cut speed, and the movement of the cutter tip. A higher aspiration pressure leads to a larger volume of fluid and vitreous being pulled into the port per cut. The driving force for removal is high and the surrounding tissue feels a large removal force, corresponding to a high traction situation. When the aspiration pressure is lower, there is less volume of fluid and tissue entering the cutter tip per cut, thus less traction.

In general, higher cutting rates (number of cuts-per-minute) allow less fluid and tissue to enter the port per cut. This allows the surgeon to remove vitreous consistently and accurately by limiting the distance the tissue is pulled with each cut. Thus, higher cutting rates are typically used close to the retina. In conjunction with cut rate, duty-cycle, port size and port shape also affect traction. These factors have fueled debate concerning the optimal method of vitreous removal. Consult recent literature articles for more information, and look to upcoming talks and articles to continue to shed light on the mechanics of vitrectomy.

The factors and effects discussed above hold when adjusting parameters for a certain cutter design and size. 25-gauge cutters have greater flow losses and lower flow than 20-gauge cutters operating at the same parameters. 25-gauge cutters are operated at higher aspiration settings (e.g., 550 mmHg) to overcome these greater flow losses and provide adequate flow. Thus, higher aspiration settings do not necessarily indicate that a 25-gauge cutter has greater traction than a 20-gauge cutter. For 25-gauge cutting, high cut speeds are important for reduced traction, and can have the added benefit of more consistent flow. The smaller portions of vitreous produced by higher cut speeds flow more easily through the small diameter cutter cannula. While the increased flow resistance and decreased flow rate of 25-gauge cutters may extend the vitrectomy time, as compared to 20-gauge, the overall 25-gauge instrumentation system has the potential to make up the differential [1].

2.8 Illumination

For 25-gauge instrumentation to be utilized intraocular, the surgeon needs illumination. As with the vitreous cutter, 25-gauge fiber optic light pipes are designed to operate through the microcannula system, and provide intraocular illumination. The primary distinction between 20- and 25-gauge light pipes is the diameter of the distal shaft, which requires a smaller fiber optic for 25-gauge light pipes.

The transmission of light from the illumination source to the eye is more complex than the infusion fluid path. For the illumination system, the smaller fiber optic associated with 25-gauge does not provide a direct restriction of light “flow” to the eye, but does affect how light is coupled into the light pipe connector. This effect may be dramatic when 25-gauge light pipes are utilized on illumination systems with optics designed for larger instrumentation. The following sections provide information on illumination systems in general, and highlight aspects that affect 25-gauge light pipe performance.

2.8.1 Terminology

An understanding of the fundamental parameters is essential in quantifying illumination in ophthalmology, especially since there has been confusion in the use of terminologies related to the surgical domain. This section addresses these fundamental parameters and terminology.

Luminance and *illuminance* are the two primary terms mentioned in the photometric domain. *Luminance* is defined as the optical energy leaving a surface, whereas *illuminance* describes the intensity of light that is falling on a surface. Imagine a sphere surrounding a light source, the energy exiting this boundary is characterized in *lumens*. If the light distribution from a point source is in all directions, then characterization is difficult. Therefore, directionality on a viewing surface is what determines the terminology.

Distribution of optical energy density on a given surface is measured by a lux-meter. For the case of quantifying output from a light pipe, the units of measure are *lux* or *lumens/area* [2]. Lamp manufacturers specify *candela* on their specification sheets, which is defined as *lumen/steradian*. It is the figure of merit of the light energy in a specific direction within the sphere which relates to a spot in the center of the beam. Higher *candela* means higher energy distribution in an area.

Other terminology is the *radiance* or *brightness* of the source, and is the amount of optical power emitted in a specific direction per unit time by a unit area of emitting surface. In a majority of light sources, only a fraction of the power emitted by the source is coupled into the optical fiber. It is also common for the medical community to liberally use *brightness* and *whiteness*, as a figure of merit to quantify light sources. This is misleading, although qualitatively it may have some credibility. *Brightness* depends on the *luminance*, which in turn is related to the *candela/area* [2] of the viewing surface. When a surgeon views, he or she views the energy reflected from a surface. It is difficult to quantify brightness, and therefore the accurate figure of merit is *lux* or *lumens*.

Whiteness on the other hand depends on the color temperature of the light source. For example, xenon lamps are whiter than incandescent lamps. When a blackbody radiates energy, it changes color with increasing temperature. The spectrum shifts from far visible (red) to short visible (blue). Therefore, high intensity discharge (HID) lamps with higher efficacy and wattage tend to produce a *whitish* light. Other factors that influence the visualization are glare, uniformity of *illuminance*, and color rendition. Color Rendering describes how an optical source depicts the colors of an object to human eyes, and how fine faint variations are revealed in color shades. The figure of merit is defined in terms of the color rendering index (CRI) which uses a scale ranging from 0 to 100%. The higher the CRI is on the scale, the better a source's color-rendering ability. One important factor is that CRI is independent of color temperature.

2.8.2 System Approach

An illumination system for ophthalmic applications is comprised of five basic building blocks as shown in Fig. 2.17. The power supply module drives the illumination source, which couples light into the fiber optic light pipe through an optical system. In the development of illumination systems, it is essential to ensure the proper operation of each module for maximum optical output. The design of the power supply module depends on its drivability, whether the system is based on current or voltage. The key to an efficient optical design depends on the illumination source module. The type of lamp, intensity, spectral signature and thermal cooling contribute to the design of this module. The optical system module consists of a combination of lens and filters that improve system coupling efficiency. Lens devices are used to focus or collimate the optical energy, and are made of shaped glass or plastic. Alternatively, a filter assists in the removal of unwanted spectral signatures, and provides safety by limiting photo toxicity or damage in the eye.

The way in which the light from the source is translated into the eye is via an optical fiber which is small enough to fit through a 20-gauge or 25-gauge cannula. This phenomenon is referred to as coupling, where the energy is transferred from a free space into an optical fiber. An optical fiber is a cylindrical dielectric waveguide that transmits light along its axis by the process of total internal reflection. The loss in the illumination system depends on each interface, and is determined through coupling efficiency, a figure of merit of the energy distribution from the input to the output. The following sections address each of the modules in detail.

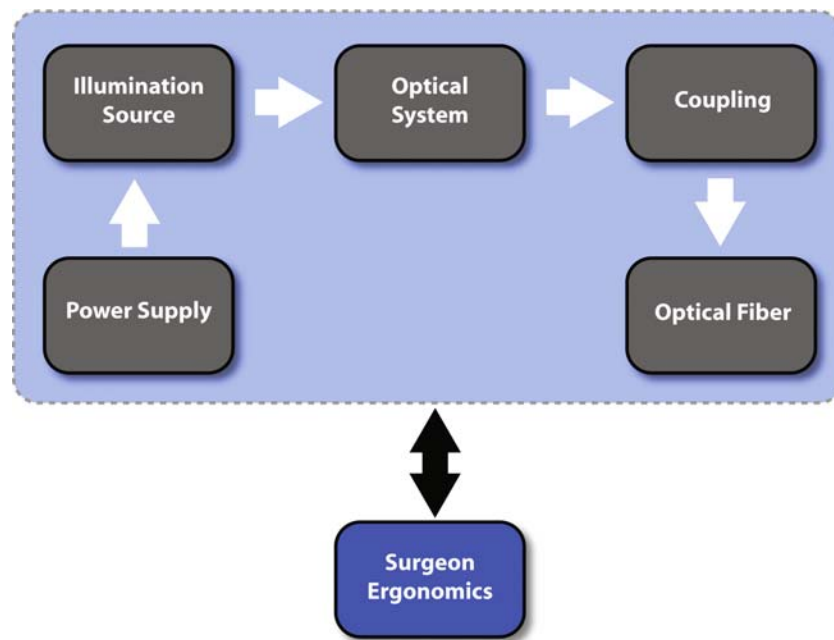


Fig. 2.17 Illumination system design overview

2.8.3 Power Supply Module

Ballast [17] is an essential component the power supply module that drives high discharge lamps that are currently used for ophthalmic lighting. A majority of high discharge lamps require a higher voltage at start, and then plateau out at a nominal lower voltage. The ballast functionality is to provide an acceptable starting voltage when the system is initially activated. Secondly, the ballast allows impedance matching, where the supply line voltage is matched with the operating voltage of the lamp under all conditions. Efficient ballast is an essential part of the illumination system, and prevents fluctuations in light output. An incorrect ballast design could lead to significant loss of energy, reduction in lamp life, incorrect light output levels and increased system cost [18]. There are two categories of ballast design: magnetic and electronic. Magnetic ballast is mainly used for fluorescent lamps, and electronic ballast is used for high-discharge lamps, which are used in ophthalmic lighting applications. Current lamps are designed with electronic ballast that converts standard 60 Hz input frequency to a higher frequency, as high as 40,000 Hz. This allows the lamp to operate at low wattage and incorporate a variable light output intensity feature. Another part of the power supply is a quick-start circuit, which assists in providing constant heating of the

filament after the bulb is activated. This allows the light source to maintain a constant spectral output signature.

2.8.4 Illumination Source

The selection of the light source is critical to the efficiency and quality of the illumination system [19]. In general, the choice of the light source depends primarily on its application. Other factors include the cost of the lamp, intensity, spectral and color issues, and whether the system needs a variable output. Incandescent, fluorescent, and high intensity discharge are categories of lamps available in the market, although new semiconductor lighting is making inroads [20]. For ophthalmic applications, high intensity discharge lamps are primarily used.

Light source selection depends on *efficacy*, a figure of merit for the conversion of electrical into optical energy. It is defined as the output lumens per input wattage, and has units of lumens per watt. The higher the efficacy, the less energy the lamp needs to operate. Parameters such as color temperature, color rendering index and efficiency are also critical. Incandescent and high intensity discharge (HID) lamps are prominent, and suitable for ophthalmology applications. HID lamps are used in the current illumination systems available, for example Photon from Synergetics Inc. (O'Fallon, MO, USA),

Millennium from Bausch and Lomb Inc. (St. Louis, MO, USA) and Accurus from Alcon Laboratories, Inc (Fort Worth, TX, USA).

HID lamps have short arcs that are generated between two electrodes under high pressure. Although short, the arc can generate high temperature, high efficacy, and long life (20,000+ h) in an efficient package. Although they are efficient, they have limitations, which may be observed in surgery. Lamp warm-up, or the time to obtain a full spectral signature with desired intensity, takes between 2–5 min. The other potential issue for HID lamps is re-striking, where if the power supply switches off, to bring it to an on state would require 15–20 min to cool the lamp before turning it on. In ophthalmic applications, re-strike is not a major problem, as the bulbs are never turned off and on from the power supply. There are four categories of HID lamps; mercury vapor, metal halide, high-pressure sodium and low-pressure sodium. We will be discussing only two HID lamps: metal halide and high-pressure sodium, as they are the primary light sources used in ophthalmology.

Metal halide lamps utilize mercury and argon gases inside the arc tube to improve efficacy and allow variable wattage of the lamp. Unfortunately, metal halides suffer from spectrum shifting with the change of voltage, and lower life than other HID lamps. Currently, metal halide lamps are used in the Millennium system from Bausch and Lomb Inc. (St. Louis, MO, USA). High-pressure sodium lamps consist of high-voltage starter ballast with an arc tube that is filled with gases such as xenon, sodium and mercury. These lamps can be used at high wattages, and have higher efficacy with minimal spectrum shifting. The disadvantage is that they require an additional cooling system, which increases cost and space requirements. Currently, xenon lamps are used in the Accurus system from Alcon Laboratories, Inc (Fort Worth, TX, USA) and the Photon light source from Synergetics Inc. (O'Fallon, MO, USA).

2.8.5 Optical System

An optical system module enhances the coupling efficiency of the illumination system with the aid of a combination of reflectors, lenses and filters. The system assists in focusing light to a desired spot with maximum energy distribution. This is achieved through lens devices which either concentrate or diverge light, and filters which assist in the removal of harmful spectral signatures. Design parameters are determined depending on the path of the light from the source. The direction of the optical energy is established by

optical system efficiency, reflective and shielding material properties. Some illumination sources utilize reflectors which redirect the light emitted from a lamp in order to achieve a desired distribution of light intensity outside of the luminaire. These reflectors are coated with either silver, anodized aluminum sheet or dichroic coatings which are effective in removing ultra-violet (UV) spectrum.

The lens system design [21] depends primarily on the directionality of the incoming optical rays. Maximum coupling efficiency is achieved if the incoming rays are parallel. There are a number of different types of lenses available for optical design. In ophthalmic lighting applications, biconvex or plano-convex lens types are employed, as they collimate the beam of light traveling parallel to the lens axis, which then, passing through the lens, converges to a spot on the axis at a certain distance behind the lens (focal length). The optical fiber is placed at the focal point for maximum coupling of energy. These types of lenses are also referred to as *positive* or *converging* lens. A combination of collimating and converging spherical lenses can increase the coupling efficiency of an optical system [22].

$$\text{Reflectivity} = R = \left(\frac{n-1}{n+1} \right)^2$$

Whenever optical energy passes through an interface, in this case an uncoated lens or filter, there is loss of energy. Therefore, optical component designers use antireflective coatings to reduce the amount of light lost to reflection at the surfaces of individual transmissive elements. Mathematically, surface reflection is predicted using Fresnel's equation for normally incident light [23]:

Reflectivity or R of uncoated glass is a function of refractive index, n ; where increased index leads to high reflectivity. The use of antireflective coatings like magnesium fluoride (MgF_2) can reduce reflection at a glass surface by approximately 2%. Increasing the layering of coatings can minimize losses by almost 50%. Therefore, the choice of lenses and their coatings is critical in reducing coupling loss.

The final element in the optical design module is a filter, which is a device that selectively transmits light with certain properties while blocking the remainder. This is essential in attempting to minimize illumination system photo-toxicity inside the eye, as it is dependent on the spectral signature. The ANSI spectrum consideration for a light source ranges from 420–690 nm. Therefore, medical illuminators use filters to selectively remove unwanted

wavelengths. These filters may be integrated into a lens, included within the optical fiber, or a combination of both to reduce toxicity in patients. The filters are either intensity-based or spectral-based.

2.8.6 Optical Fiber

The light from the source is translated into the eye through an optical fiber based light pipe. An optical fiber is a dielectric waveguide, cylindrical in shape, which transmits light parallel to its axis. It consists of a core surrounded by a cladding layer and jacket for protection. There are two parameters used to distinguish fiber types, mode and index. We assume step index fiber for simplicity, where the fiber refracts the light sharply at the point where the cladding meets the core material. In addition, there are two categories of fibers: glass and plastic [24]. Glass fibers made of silica have resistance to high temperatures, improved transparency, chemical durability and low attenuation or loss. Mechanical durability is the primary disadvantage, and may be rectified by using plastic fibers that are made from PMMA (poly-methyl-metha-acrylate). Polymer fibers are inexpensive and flexible. Although they have a high loss over long distances, this loss is minimal for light-pipe applications. Currently, most light pipes are designed of plastic fibers.

We are going to discuss the basic principle of light transmission, and not the modes and index, as it is outside the scope of this chapter.

2.8.6.1 Principle of Total Internal Reflection

Figure 2.18 shows the light traversing through an interface separated by two distinct media: n_{core} , index of the core and n_{clad} , the index of the cladding. The index parameters are also known as index of refraction, and are defined as the ratio of the speed of light in a vacuum. For the light to transmit, $n_{\text{core}} > n_{\text{clad}}$ should be satisfied. Part of the light changes direction either through refraction or reflection when traversing from one media to another. Snell's law, shown below, defines how much bending takes place when the light strikes the respective boundary. Let's analyze the light traveling from the core to the cladding.

$$n_{\text{core}} \sin \phi_1 = n_{\text{clad}} \sin \phi_2$$

or

$$n_{\text{core}} \cos \alpha_1 = n_{\text{clad}} \cos \alpha_2$$

The rays traveling from a medium of lower refractive index into a medium of higher refractive index bend toward the normal. Vice versa, if the light travels from a medium of higher refractive index to a medium of lower refractive index, it is bent away from the normal [25]. Therefore, a light ray launched into the core of an optical fiber propagates through the principle of total internal reflection, a condition when the refracted ray is reflected back completely as in Fig. 2.19. Incident light striking the interface is bent away from the normal; the departing angle

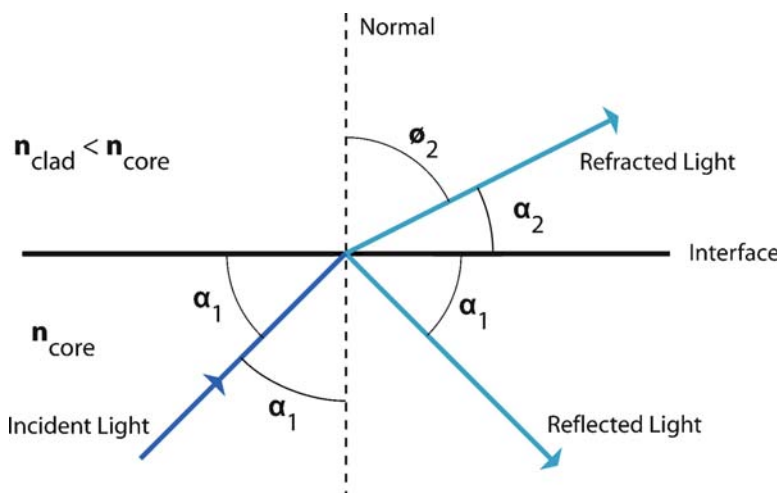


Fig. 2.18 Transmission of light rays through the core-clad fiber optic interface

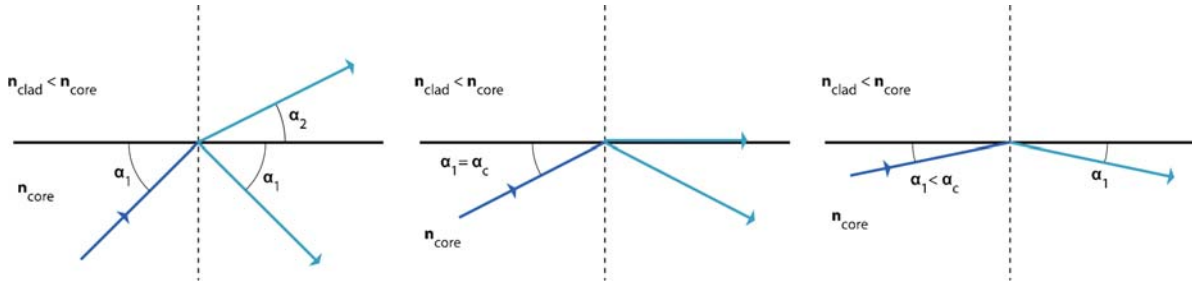


Fig. 2.19 Condition for ray propagation through core-clad interface

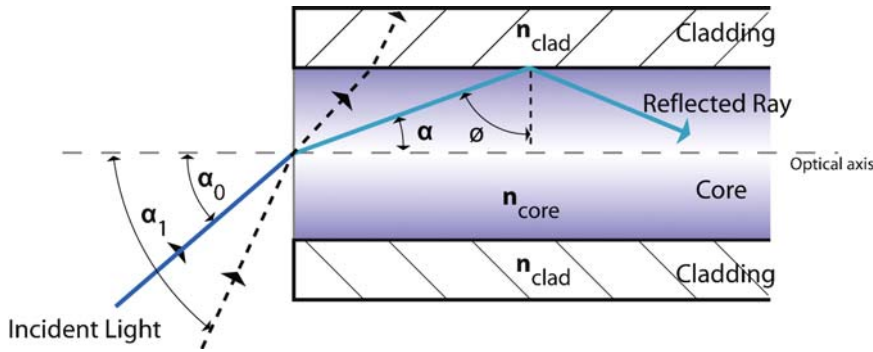


Fig. 2.20 Ray propagation through an optical fiber

(α_2) is less than α_c . If the departing angle approaches 0° for some critical incident angle α_c , the incident angle is smaller than the critical angle, which leads to total internal reflection. Therefore, the condition for minimum loss at the fiber core-clad interface occurs when $\alpha_1 < \alpha_c$.

A significant parameter that determines the coupling efficiency of the light pipe is the numerical aperture (NA), as shown in Fig. 2.20, where the light is striking the air/fiber interface. The incident striking angle is defined by α_0 to α_1 . So which angle leads to maximum coupling? This light-gathering angle is determined by the NA. Typical values of index of refraction for air ($n_{\text{air}} = 1$), core ($n_{\text{core}} = 1.5$) and clad ($n_{\text{clad}} = 1.46$).

$$\begin{aligned} \text{Numerical Aperture} = NA &= n_{\text{air}} \sin \alpha_{0\text{MAX}} \\ &= n_{\text{core}} \sin \alpha_c = \sqrt{(n_{\text{core}}^2 - n_{\text{clad}}^2)} \end{aligned}$$

A dimensional number, it lies between 0 and 1. If $NA = 0$ ($\alpha_{0\text{MAX}} = 0^\circ$), it means that the fiber gathers no light, and if $NA = 1$ ($\alpha_{0\text{MAX}} = 90^\circ$), the fiber gathers all the light that falls onto it. Current fibers used in light pipes have an NA of approximately 0.4–0.6.

A higher NA fiber captures increased light into the fiber. Consider two light pipes, one with a 1-mm diameter

fiber with $NA = 0.5$, and one with a 0.5-mm diameter fiber with $NA = 0.7$. Assume the spot size is 0.4 mm. The 0.5-mm diameter light pipe would capture more light than the 1-mm diameter light pipe. Therefore, it is important to note the role the NA of the fiber plays, and it is the parameter to look for when investigating optical fibers. The size of the fiber also plays a role in coupling, but a larger diameter fiber with a lower NA has a lower coupling capability than a smaller diameter fiber with a higher NA.

2.8.7 System Loss

The efficiency of the illumination system, or the output of a light pipe, depends on its *coupling efficiency*, a measure of the power emitted from the optical source which can be coupled into the fiber. System efficiency dependence is addressed by two fundamental issues. First, launching of the optical energy from the illumination source into a fiber, and second, the effect of the coupling or energy transfer from the free space to the enclosed space of a fiber. The amount of energy launched from the source into a fiber depends on the optical properties of both the source and the fiber, in addition to the radiance of the source. Therefore,

optical system designers maximize the efficiency by tweaking the parameters.

Coupling efficiency is defined as the ratio of power coupled into the optical fiber P_{OF} to the power emitted by the illumination source P_{IS} . The higher the coupling efficiency, the higher is the coupled output power.

$$\text{Coupling Efficiency} = \eta = \frac{P_{OF}}{P_{IS}}$$

where:

P_{IS} = power emitted by illumination source

P_{OF} = power coupled into the optical fiber

There are a number of factors that influence illumination system loss[25], and thus are critical to the design. These include numerical aperture, core size, radiance, power distribution, and spot size. For the fiber optic, coupling losses may also be due to the fiber position, lateral and angular alignment, refractive index profiles of core/clad, and poor termination of the fiber edge. A smooth and clean fiber with its faces at a 90° angle to the fiber axis is of paramount importance.

A significant amount of coupling loss occurs at the air/fiber interface. Ineffective capturing of the energy from the source, losses due to reflection from the lens system and inefficiency of the optical design also contribute to coupling losses. In addition, an illumination system designed for a particular technology, for example 20-gauge, may be ineffective with another technology, 25-gauge, as the fiber dimensions change and reduce performance, as discussed in the Optical Fiber section.

One issue worth particular mention, especially in the discussion of 20- and 25-gauge instrumentation, is spot size and the effect of spot size on coupling performance. Consider a condition where the optical power is launched into a step index fiber. The source is symmetric with an even brightness and surface area. The optical rays from an

illumination source with parallel output (parabolic reflector with the source) traverse through a lens system and converge to a point with a known spot diameter. The total power concentrated at the spot is P_{SPOT} with an area of A_s or $(2\pi R_s)$, R_s being the radius of the emitting area. The area of the fiber core is A_{OF} with R_{OF} as its radius. Assume the fiber is placed in an optimum alignment position for maximum power transfer with a numerical aperture of NA . The power at the source with radiance B_{IS} is given by:

$$\text{Source Power} = P_{IS} = \pi R_s^2 B_{IS}$$

where:

R_s = radius of emitting area

B_{IS} = source radiance

So, what is the effect of the spot size and fiber area on the coupling? Let us consider two cases; first, when the spot diameter is smaller than the fiber core diameter, and second, when the spot diameter is larger than the fiber core, as shown in Fig. 2.21. Please note the derivations are outside the scope of this chapter. When the spot diameter is smaller than the fiber core diameter, the power launched into the fiber is approximated by:

$$P_{COUPLED} = P_{IS} (NA)^2 \quad \text{when } R_{SPOT} \leq R_{OF}$$

where:

R_{SPOT} = radius of spot

R_{OF} = fiber core radius

When the spot diameter is larger than the fiber core diameter, the power launched into the fiber is approximated by:

$$P_{COUPLED} = \left(\frac{R_{SPOT}}{R_{OF}} \right)^2 P_{IS} (NA)^2 \quad \text{when } R_{SPOT} \geq R_{OF}$$

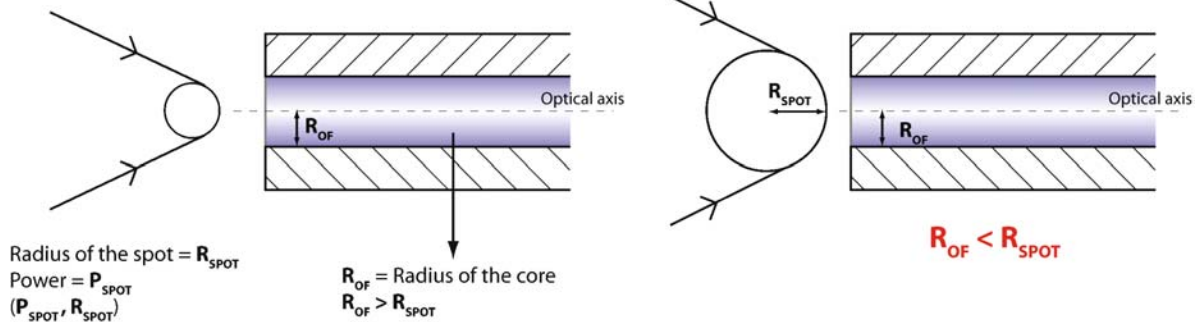


Fig. 2.21 Graphical representation of spot – fiber core sizes

For the case where the fiber core end area is less than the spot diameter, the coupled power is reduced with respect to a ratio of the radii squared. Thus, the use of a 25-gauge light pipe on a system with a spot size optimized for a larger fiber may operate with reduced performance. This is important, as the spot size can only be reduced to an extent through a lens system. As ophthalmic surgery moves towards smaller instrumentation and smaller fibers, the design of the optical system is critical, challenging and essential in improving light intensity out of a light pipe.

2.8.8 System Compatibility

In terms of illumination, 25-gauge instrumentation is not completely compatible with systems designed for 20-gauge. Optical systems are built for a specific technology, and decrease in performance if there is an alteration, as seen in 25-gauge systems. The optical system performance depends on numerical aperture, core size, radiance, power distribution and spot size. Other factors include fiber position, lateral and angular alignment, refractive index profiles of core and clad and poor termination of the fiber edge [26]. Currently, optical engineers are redesigning high efficient systems for

25-gauge ophthalmic applications. Approaches include novel lens and reflector design with efficient fiber-coupling techniques for improved light output. In the future, provisions could be made during the design to account for smaller instrumentation.

2.9 Instrument Rigidity

One of the mechanical challenges associated with small diameter instruments is instrument rigidity. As the diameter of the instrument decreases, the rigidity also decreases, causing increased flexing in 25-gauge instrument shafts. This is best understood by examining the bending equations that govern the displacement of the instruments under a load. The amount of displacement of a beam held with a fixed wall constraint is given by the equation below:

$$\omega_{\max} = \omega(L) = -\frac{PL^3}{3EI}$$

Where ω_{\max} is maximum displacement, L is the length of the beam, E is the modulus of elasticity, and I is the area moment of inertia of the beam (or second moment of area). The length of the shaft (L) for the case of an instrument inserted through an ESA microcannula is the distance from the cannula to the instrument handle. Thus, the length of shaft exposed to bending varies with the instrument insertion depth. A diagram of the beam and plot of beam displacement is shown in Fig. 2.22.

Summary for the Clinician

- The principal differences between the 25- and 20-gauge infusion line and vitreous cutter are found at the distal tubes (cannulas) that enter the eye. When the inner diameter of the instrument is reduced, a larger pressure differential is required to maintain equivalent flow rates.
- In 25-gauge vitrectomy cases, higher pressures are typically required to produce similar flow rates to corresponding 20-gauge procedures.
- Higher vacuum pressure and/or greater intraocular pressure (i.e., a higher infusion pressure) will result in a higher flow rate.
- For 25-gauge cases, an aspiration vacuum setting of 550 mmHg is a typical operating parameter
- Traction is an important dynamic of vitrectomy. It is the pulling force that is applied to tissue due to aspiration flow. Traction is necessary for vitreous and other material to enter the cutter port.
- Traction is typically controlled by the surgeon varying aspiration pressure, cut speed, and the movement of the cutter tip. Higher cutting rates are typically used close to the retina.

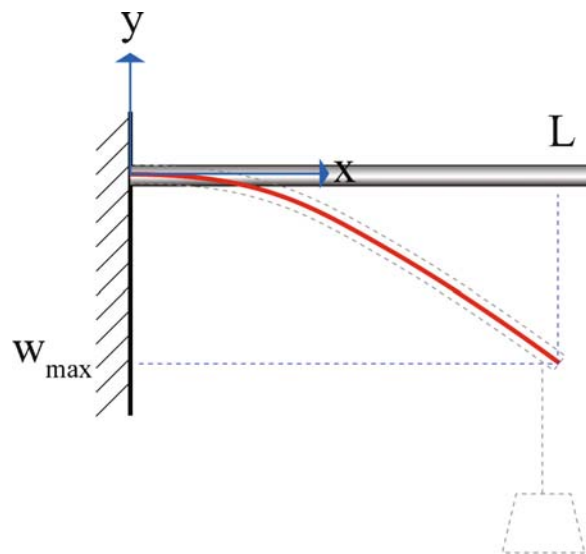


Fig. 2.22 Beam bending

From the equation, it may be seen that the three methods to reduce shaft deflection (increase rigidity) are: (1) to decrease the instrument length exposed to a bending load (L), (2) increase the modulus of elasticity (E), or (3) increase the area moment of inertia (I). The parameter having the greatest impact on shaft rigidity is the length of the shaft. Shaft deflection is proportional to the third power of the length.

The modulus of elasticity is a material property. Most instrument shafts use stainless steel, which has a modulus of elasticity of approximately 200 GPa. This is fairly high compared with other materials. Altering the shaft material to increase the modulus of elasticity is possible, but it is difficult to achieve significant gains over stainless steel. Stiffer materials may also reduce the toughness of the instruments, increasing the likelihood of shaft fracture.

The area moment of inertia is related to the shaft cross-sectional area and the distance the area is from the bending centerline. Mathematically, it is expressed as: where:

$$\text{Area moment of inertia} = I = \int y^2 dA$$

dA = elemental area

y = perpendicular distance from bending axis to dA

This illustrates that the further the mass is from the center of the instrument, the higher the area moment of inertia. For the specific case of a tube of circular cross-section, the area moment of inertia with respect to its central axis is:

$$I = \frac{1}{4} \pi (r_{\text{outer}}^4 - r_{\text{inner}}^4)$$

The area moment of inertia is ultimately limited by the outer shaft diameter (25-gauge) and the wall thickness of the tubing. The wall thickness is limited by the inner diameter required for any functional components of the instrument (e.g., inner cutter mechanism, fiber optic, forceps). Minimizing wall thickness allows a larger fiber or greater cutter aspiration, but also reduces instrument rigidity. The length of the instrument shaft is governed by the diameter of the eye. The surgeon needs to have full access to the interior of the eye for almost all instruments.

As shown above, reducing the length of the shaft exposed to a bending load has the greatest impact on shaft rigidity. For example, a light pipe may employ a small stiffening sleeve on the light pipe shaft to reduce the length of 25-gauge shaft exposed between the instrument handle and cannula hub. Since the light pipe is used in conjunction with the other instruments, a stiffer light

pipe provides increased ability to move the eye during surgery. Finger-positioning techniques may also be used to support instrument shafts. By positioning a finger on the instrument shaft, the surgeon can provide increased support. This may be especially useful when the instrument is inserted to a shallow depth with a large length exposed to bending.

2.10 Discussion

The sutureless 25-gauge pars plana vitrectomy reduces the postoperative inflammation at sclerotomy sites, thus reducing patient discomfort after surgery and hastening postoperative recovery [1–8]. The smaller incisions also result in less vitreous incarceration to the scleral wound, therefore possibly reducing the risk of peripheral retinal tears and retinal detachments. However, because of the small size of the instruments, there are engineering development challenges and trade-offs associated with 25-gauge instruments. Many critical intraoperative situations require surgeons to decide on microsurgical system parameters and instrument technique. With an understanding of the performance differences between 20 and 25-gauge instrumentation, surgeons will be better prepared to select the most appropriate system for the case and adjust system parameters in order to result in a safe surgical procedure.

This knowledge will also assist the surgeon in evaluating performance differences between existing systems and new instrumentation and techniques, such as 23-gauge instrumentation utilizing tunneling sclera incisions. The increased diameter of 23-gauge instrumentation (relative to 25-gauge) provides the potential for stiffer instruments, higher maximum volume flow rates, and greater maximum endoillumination. However, the larger 23-gauge wounds require an oblique incision that tunnels through the sclera to allow a sutureless close. This incision technique and 23-gauge instrumentation are just beginning to be evaluated by the vitreoretinal community.

The majority of 25-gauge instrumentation currently available has been developed by modifying the design of existing 20-gauge instruments, and is being utilized on microsurgical systems optimized for 20-gauge. While many of the engineering development challenges of 25-gauge instruments may be attributed to their small diameter, there are a significant number of trade-offs associated with utilizing 25-gauge instruments on equipment designed for larger instruments. As new equipment is developed, optimized for both small and large diameter instrumentation, the performance of transconjunctival 25-gauge instrumentation will continue to improve.

References

1. Born M, Emil W (1999) Principles of optics: electromagnetic theory of propagation, interference and diffraction of light, 7th expand edn. Cambridge University Press, Cambridge
2. Chen JC (1996) Sutureless pars plana vitrectomy through self-sealing sclerotomies. *Arch Ophthalmol* 114(10):1273–1275
3. DeBoer C et al (2006) Vitreous removal rates and high-speed video analysis of 25-gauge vitrectomy cutters. ARVO Annual Meeting (2006) Abstract
4. Eckardt C (2005) Transconjunctival sutureless 23-gauge vitrectomy. *Retina* (Philadelphia, Pa.) 25(2):208–211
5. Fischer RE, Biljana T-G (2000) Optical system Design. McGraw Hill, New York
6. Flesch PG (2006) Light and light sources: high-intensity discharge lamps, 1st edn. Springer, Berlin New York Heidelberg
7. Fujii GY et al (2002) A new 25-gauge instrument system for transconjunctival sutureless vitrectomy surgery. *Ophthalmology* 109(10):1807–1812; discussion 1813
8. Fujii GY et al (2002) Initial experience using the transconjunctival sutureless vitrectomy system for vitreoretinal surgery. *Ophthalmology* 109(10):1814–1820
9. Hasumura T et al (2000) Retinal damage by air infusion during vitrectomy in rabbit eyes. *Invest Ophthalmol Vis Sci* 41(13):4300–4304
10. Hirata A et al (2000) Effect of infusion air pressure on visual field defects after macular hole surgery. *Am J Ophthalmol* 130(5):611–616
11. IESNA Light Sources Committee (1998) IESNA guide to choosing light sources for general lighting. Illuminating Engineering Society of North America, New York
12. Jackson T (2000) Modified sutureless sclerotomies in pars plana vitrectomy. *Am J Ophthalmol* 129(1):116–117
13. de Juan E Jr, Hickingbotham D (1990) Refinements in microinstrumentation for vitreous surgery. *Am J Ophthalmol* 109(2):218–220
14. Keiser G (2000) Optical fiber communications, 3rd edn. McGraw-Hill, Boston, MA
15. Kwok AK et al (1999) Modified sutureless sclerotomies in pars plana vitrectomy. *Am J Ophthalmol* 127(6):731–733
16. Ladd BS et al (2003) Force comparison of air currents produced by a standard and modified infusion cannula. *Retina* 23(1):76–79
17. Lam DS et al (2000) Sutureless pars plana anterior vitrectomy through self-sealing sclerotomies in children. *Arch Ophthalmol* 118(6):850–851
18. López-Higuera JM (2002) Handbook of optical fibre sensing technology. Wiley, New York
19. Mohan N, Tore MU, William PR (2003) Power electronics: converters, applications, and design, 3rd edn. Wiley, Hoboken, NJ
20. Oshitari K et al (2001) Evaluation of retinal damage induced by air/fluid exchange using a trypan blue inclusion test in rabbits. *Am J Ophthalmol* 131(6):814–815
21. Rahman R et al (2000) Self-sealing sclerotomies for sutureless pars plana vitrectomy. *Ophthalmic Surg Lasers* 31(6):462–426
22. Sabersky RH (1999) Fluid flow: a first course in fluid mechanics, 4th edn. Prentice Hall, Upper Saddle River, NJ
23. Smith WJ (2005) Modern lens design, 2nd edn. McGraw-Hill, New York
24. Tomal, DR, Neal SW (2004) Electronic troubleshooting, 3rd edn. McGraw-Hill, New York
25. Vo-Dinh T (2003). Biomedical photonics handbook. CRC Press, Boca Raton, FA
26. Yonemura N et al (2003) Long-term alteration in the air-infused rabbit retina. *Graefes Arch Clin Exp Ophthalmol* 241(4):314–320

Vitreo-retinal Surgery

Progress III

Rizzo, S.; Patelli, F.; Chow, D. (Eds.)

2009, XVIII, 234 p. 50 illus., 31 illus. in color., Hardcover

ISBN: 978-3-540-69461-8